The use of artificial neural networks (ANN) for modeling of adsorption of Cr(VI) ions

Biswajit Singha, Nirjhar Bar, Sudip Kumar Das*

Department of Chemical Engineering, University of Calcutta, 92, A. P. C. Road, Kolkata 700009, India
Email: drsudipkdas@vsnl.net

ABSTRACT

In this study, an artificial neural network (ANN) based techniques is applied for the prediction of the percentage removal of Cr(VI) ions from aqueous solution using eight different natural biosorbents. The effects of operating parameters such as initial pH, initial Cr(VI) ion concentration, adsorbent dosages, and contact time are studied to optimize the conditions for maximum removal of Cr(VI) ions. The ANN with a single hidden layer trained with Levenberg-Marquardt algorithm predicted the percentage removal of Cr(VI) ions from aqueous solution accurately.

Keywords: Cr(VI) ions; Saw dust; Coconut shell; Backpropagation; Levenberg-Marquardt

1. Introduction

Pollutants like toxic heavy metals and dyes are released from different types of industries to the environment causing different disease and disorder. Cr(VI) is one of the most important toxic heavy metal discharged from various industries including mining, tanning, cement, production of steel and other metal alloys, electroplating operations, photographic material and corrosive painting industries [1,2]. It is carcinogenic, mutagenic, and toxic; thus, its presence in the environment poses a significant threat to aquatic life as well as public health [3]. The maximum permissible limit of Cr(VI) for the discharge to inland surface water is 0.1 mg/L and in potable water is 0.05 mg/L [4,5]. The Ministry of Environment and Forest, Government of

India has set minimal national standards of 0.1 mg/L for safe discharge of effluent containing Cr(VI) in surface water [6]. In order to comply with this limit, industries have to treat their effluents to reduce the Cr(VI) concentration in wastewater to acceptable levels. In waste water treatment, various technologies are available such as chemical precipitation, ion exchange, electrochemical precipitation, solvent extraction, membrane separation, concentration, evaporation, reverse osmosis, emulsion pertraction, adsorption, etc. [7]. Among these technologies, adsorption is a user-friendly technique for the removal of heavy metals. This process includes the selective transfer of solute components in the liquid phase onto the surface or onto the bulk of solid adsorbent materials.

In last two decades artificial neural network (ANN) models have been extensively studied in different fields of engineering, finance, etc. with a

---

*Corresponding author.

basic objective of achieving human like performance. The neural networks are powerful tools to identify underlying highly complex relationships from input–output data [8]. ANN derived from the biological counterparts, and based on the concept that a highly interconnected system of simple processing elements, known as nodes or neurons, enables to learn highly complex nonlinear interrelationships existing between input and output variables of the data-set.

In ANN model of system, feed-forward architecture, namely, multilayer perception, MLP is most commonly used. This network consists of at least three layers, namely, input layer, one or several hidden layers, and output layer. Each layer consists of a number of elementary processing units known as neurons. Each neuron in the input is connected to its hidden layer through weights. Also, there is connection between hidden and output layers. When an input is introduced to the neural network, the synaptic weights between the neurons are simulated and these signals propagate through layers and the output result is formed. The main objective is to form the output by the network in such a way that it should be close to the expected output. The weights between the layers and the neurons are modified in such a way that next time the same input will provide an output that are closer to the expected output. Various algorithms are available for the training of the neural networks. Feed-forward backpropagation (BP) algorithm is the most versatile and robust technique, which provides the most efficient learning procedure for MLP networks. This algorithm is especially capable of solving predictive problems [9]. The ANN contain hidden layer(s) that have the ability to deal robustly with very complex and nonlinear problems. The number of hidden layers corresponds to the complexity of the problem. Single hidden layer ANN creates a hyper plane. Two hidden layer networks combine hyperplanes to form convex decision areas and three hidden layer ANNs combine convex decision areas to form convex decision areas that contain concave regions [10]. The convexity or concavity of the decision region indicates roughly to the number of unique inferences that are performed on the input variables to give the desired output. Barnard and Wessels [11] pointed out that increasing the number of hidden layers enables a trade-off between smoothness and closeness-of-fit. The greater number of hidden layers improves the closeness-of-fit while a smaller number of hidden layers improve the smoothness or extrapolation capability of the ANN. White [12] indicated that single hidden layer with arbitrarily large quantity of neurons is capable of modeling accurately, whereas Walczak [13] observed that two hidden layer networks are better

than the single hidden layer network for specific problem. Bansal et al. [14], and Tamura and Tateishi [15] observed that the single hidden layer can solve most of the problems for more input variables and outputs. Recently, researchers have successfully modeled a three layer feed forward BP network to predict the removal of Cu(II) from industrial leachate by pumice [16] and Zn(II) from hazelnut shell [17].

The present paper deals with a development of a more general and system-independent neural network based on MLP having a single hidden layer trained with BP and Levenberg-Marquardt (LM) algorithms for the prediction of the percentage removal of Cr(VI) from aqueous solution using eight different bioadsorbents under different operating conditions using four different transfer functions in a single hidden layer. The details of the adsorption study of these adsorbents are reported in our earlier publications and the relevant experimental data are taken for this ANN analysis [18,19].

2. Experimental methods

2.1. Preparation of adsorbents

Saw dust of teakwood origin, neem bark, rice straw, rice bran, rice husk, hyacinth roots, neem leaves, and coconut shell were used for Cr(VI) ions removal from aqueous solution. All the adsorbents were collected from local area near Kolkota, West Bengal, India.

Firstly, the coconut shell was crashed in a roll crusher and then grinded. The saw dust, neem bark, neem leaves, and coconut shell were treated with $0.1\,N$ NaOH to remove lignin-based color materials followed by treatment with $0.1\,N$ H_2SO_4. Rice straw, rice bran, rice husk, and hyacinth roots were boiled for $6\,h$ to remove color materials. Finally, all the adsorbents were washed with distilled water several times and dried at $105°C$ for $6\,h$ to remove the adherent moisture. After drying, all the adsorbents were sieved to obtain particle size of $250–350\,\mu m$.

2.2. Reagents and equipment used

The necessary chemicals used in the experiment were of analytical grade and obtained from E. Merck Limited, Mumbai, India. The pH of the solution was measured with a EUTECH make digital microprocessor-based pH meter previously calibrated with standard buffer solutions. UV-Spectrophotometer (U-4100 spectrophotometer, Hitachi, Japan) was used to determine the Cr(VI) ions content in standard and

treated solutions after adsorption experiments. FT-IR (Jasco FT/IR-670 Plus) studies were carried out to determine the type of functional group responsible for Cr(VI) ions adsorption. Surface area was measured on micromeritics surface area analyzer (ASAP2020). Moisture content determination was carried out with a digital microprocessor based moisture analyzer (Metteler LP16). The point of zero charge (pHpzc) was determined by solid addition method [20]. All the characteristics of the biosorbents are reported in Table 1.

2.3. Preparation of standard Cr(VI)ion solution

The stock solution containing 1,000 mg/L of Cr(VI) ions was prepared by dissolving 3.73 g of A. R. grade $K_2CrO_4 \cdot 2H_2O$ in 1,000 ml double distilled water. The required initial concentration of Cr(VI) standard solution was prepared by appropriate dilution of the above stock Cr(VI) solution.

2.4. Batch adsorption studies

Using the necessary adsorbents in a series of 250 ml stopper conical flask containing 100 ml of desired concentration of Cr(VI) ion solution batch adsorption were carried out. The pH of the solution was monitored by adding 0.1 N HCl or 0.1 N NaOH solution as required. Then, the flasks were shaken for the desired contact time in an electrically thermostated reciprocating shaker with 120–125 strokes/minute at 30℃. Cr(VI) concentration was estimated by drawing conical flask from shaker at regular intervals of time to find the equilibrium when the concentration is constant against time The contents of the flask were then

filtered through filter paper (Whatman No. 1). UV-visible spectrophotometer was employed to determine the remaining Cr(VI) concentration in the sample using 1,5-diphenylcarbazide method as laid down in standard methods for examination of water and wastewater, 1998 edition, APHA, AWWA, WEF [21]. The removal efficiency of Cr(VI) ions by different biosorbent from aqueous solution was calculated using following equation,

Percentage removal of Cr(VI) ions

$$= \frac{(C_0 - C_t)}{C_0} \times 100\% \tag{1}$$

where C_0 is the initial Cr(VI) ion concentration and C_t is the concentration at any time t. All the investigation were carried out in triplicate to avoid any discrepancy in experimental results with the reproducibility and relative deviation of the order of ± 0.5 and $\pm 2.5\%$, respectively.

2.5. ANN Structure and its Optimization Procedure

Fig. 1 presents the schematic diagram of the ANN. Soulié [22] pointed out that the selection of the input variables is the most important and a very complex task for the ANN. Pakath and Zaveri [23] claimed that ANNs are highly dependent on the specification of the input variables. However, in general, input variables are routinely misspecified by the ANN developers [24]. So, the first step is to determine the optimal set of input variables to perform the ANN in a best possible way. Researchers [13,25,26] have clearly indicated that the requirement for the extensive knowledge acquisition is necessary for properly utilizing the domain experts to specify the ANN input variables. Smith [27] pointed out that the ANN input variables should be predictive but not correlated in nature, because the correlated variables degrade the ANN

Table 1
Different physical characteristics of natural adsorbents

Adsorbents	Surface area (m²/g)	Moisture content (%)	Point of zero charge	Ash content (%)
Saw dust	3.85	8.63	3.90	12.35
Neem bark	3.47	9.23	4.50	10.62
Rice straw	1.21	7.26	6.85	9.40
Rice bran	0.12	10.68	6.10	11.72
Rice husk	0.54	9.02	6.05	11.80
Hyacinth roots	5.78	11.25	6.59	10.74
Neem leaves	0.57	8.33	6.94	13.58
Coconut shell	0.52	6.16	6.62	9.23

Fig. 1. Schematic diagram of BP network.

performance by interacting with each other as well as other elements to produce a biased effect. Lenard et al. [28] observed that the reduction of the input set size by 50%, i.e. eight—four input variables improved the performance of the ANN by 1.2–9%. Whereas, Jain and Nag [29] indicated that the reduction of input variables did not improve the ANN performance, although they used statistical measure of the predictiveness and eliminated all the correlated variables.

The input variables for the modeling of the Cr(VI) removal are as follows:

(1) Name of the adsorbent
(2) Initial pH
(3) Initial concentration of Cr(VI)
(4) Adsorbent dosage

The equilibrium contact time is taken for all cases and is shown in Table 2. Hence, it is not taken as an input variable. The output variable is the percentage removal of Cr(VI). Initially, the experimental data, i.e.

Table 2
Optimum operating conditions obtained in the batch process

Adsorbent	pH	Cr(VI) concentration (mg/L)	Contact time (min.)	Adsorbent dosage (g/L)
Saw dust	3	50	240	10
Neem bark	3	50	240	10
Rice straw	2	25	180	10
Rice bran	2	25	300	10
Rice husk	1.5	25	360	10
Hyacinth roots	2	25	240	10
Neem leaves	2	25	240	10
Coconut shell	2	25	240	10

input and output are randomized. The first 60% of data-points are used for training, the next 20% for cross-validation, the next 10% for testing, and the rest used for prediction. Generalized delta-rule algorithm is used for the BP for this particular network. A linear function is used in the output layer.

$$y_i = x_i + b \qquad (2)$$

Four different transfer functions were used in a hidden layer and are shown in Table 3. Here, β is the gain and it is used to control the steepness of the transfer function. The value of β is mostly unity. The general working principle of the ANN using BP algorithm is as follows:

(1) First, the output is generated.
(2) The generated output is then compared with the desired output.
(3) The deviation in step (2) is the error and this error is passed to the BP component, which adjusts the weights of the network for training.
(4) The maximum number of epochs are kept 32,000.
(5) The initial learning rate and the momentum coefficient used are 0.7 and 1.0, respectively.
(6) The stopping criteria for the BP process (1) till the error is $\leqslant 0.001$, or (2) if there is no improvement of the value of MSE for 20,000 epochs.

The synapse that connects the hidden layer to the input layer and the synapse that connects the hidden layer to the output layer adjust the weights and learning rates automatically to reduce the error. It is always desired that the number of processing elements in the hidden layer must be kept minimum to reduce the complexity of the network. In the hidden layer, the numbers of nodes are optimized by varying the

Table 3
Optimum number of processing elements in the hidden layer for four different transfer functions

Transfer function in hidden layer	Equation	Optimum number of processing elements in the hidden layer	
		BP	LM
Transfer function 1	$y = \tanh \beta x = \frac{e^{\beta x} - e^{-\beta x}}{e^{\beta x} + e^{-\beta x}}$	5	24
Transfer function 2	$y = \beta x$ Where $\begin{array}{l} \beta x = 1 \text{ for } \beta x > 1 \\ \beta x = -1 \text{ for } \beta x < -1 \end{array}$	16	21
Transfer function 3	$y = \beta x$ Where $\begin{array}{l} \beta x = 0 \text{ for } \beta x < 0 \\ \beta x = 1 \text{ for } \beta x > 1 \end{array}$	20	12
Transfer function 4	$y = \frac{1}{1 + e^{-\beta x}}$	9	12

number from 1 to 25, and for each case, the MSE was calculated.

The LM algorithm is a second-order learning algorithm. For training using LM algorithm in the hidden and output layer, the user has to set the initial value of the network parameter λ, i.e. 0.01. In the hidden layer, the numbers of nodes are optimized by varying the number from 1 to 25, and for each case, the MSE was calculated.

The number of nodes for which the value of the cross-validation MSE is minimum, is considered to be optimum. The optimum numbers of nodes are given in Table 2. Each run was set for 32,000 epochs when BP algorithm was used and was set for 300 epochs when LM algorithm was used. A similar procedure was also reported in the literature [30,31].

3. Result and discussion

3.1. Optimum operating condition

The pH of the solutions has an important variable governing metal adsorption. In general, the adsorption of cation is favored at $pH > pH_{PZC}$. The effect of initial pH on the adsorption process is represented in Fig. 2. At very low pH, chromium ions exist in the form of $HCrO_4^-$, while in the increase in pH up to $pH = 6$, different forms, such as $Cr_2O_7^{2-}$, $HCrO_4^-$, and $Cr_3O_{10}^{2-}$, coexist, of which $HCrO_4^-$ predominates. As pH increases, the equilibrium is shifted from $HCrO_4^-$ to

Fig. 2. Effect of pH on the adsorption of Cr(VI) (metal concentration: 50 mg/L for saw dust and neem bark, 25 mg/L for other adsorbents; adsorbent dosage: 10 g/L; and contact time: 5 h for saw dust, neem bark, neem leaves, 6 h for coconut shell, 7 h for rice straw, rice bran, rice husk, and hyacinth roots).

CrO_4^{2-} and $Cr_2O_7^{2-}$ [32]. At very low pH values, the surface of the adsorbent would be surrounded by the H_3O^+ ions, which enhance the Cr(VI) interaction with binding sites of the biosorbent by greater attractive forces. As the pH increased, the overall surface charge on the biosorbents became negative and the adsorption decreased [2].

The following equilibrium may be written in aqueous solutions [33].

$$H_2CrO_4 \ \leftrightarrow \ HCrO_4^- + H^+ \quad K_1 = 1.21 \tag{3}$$

$$Cr_2O_7^{2-} + H_2O \ \leftrightarrow \ 2HCrO_4^- \quad K_2 = 35.5 \tag{4}$$

$$HCrO_4^- \ \leftrightarrow \ CrO_4^{2-} + H^+ \quad K_3 = 3 \times 10^{-7} \tag{5}$$

where K's are the equilibrium constant. The adsorption of Cr(VI) ion was not significant at pH values more than 6 due to dual complexation of the anions (CrO_4^{2-}, $Cr_2O_7^{2-}$ and OH^-) to be adsorbed on the surface of the adsorbents, of which OH^- predominates [34]. The optimum pH for the adsorption process is shown in Table 2.

The percentage removal of Cr(VI) ions increases with the increase in contact time.

The biosorption considered in all cases is of two phases: a primary rapid phase and a secondary slow phase. The initial rapid phase is indicated to give away a very slow approach to equilibrium and is accounted for the major part in the total Cr(VI) ions sorption. The secondary slow phase has indicated that the adsorption process has reached equilibrium. The equilibrium time for the adsorption of Cr(VI) were 3 h for rice straw; 4 h for saw dust, neem leaves, hyacinth roots, neem leaves and coconut shell, 5 h for rice bran; and 6 h for rice husk.

The percentage removal of Cr(VI) ion decreases with the increase in initial Cr(VI) ion concentration and is shown in Fig. 3. At the lower concentration, all the Cr(VI) ions in the solution reacted with the binding sites and thus facilitated almost complete adsorption. At higher concentration, more Cr(VI) ions were left unadsorbed in the solution due to the saturation of the binding sites. This indicates that the energetically less favorable sites become involved with increasing Cr(VI) ion concentration in aqueous solutions [35,36].

The effect of adsorbent dosage for the removal of Cr(VI) ion from aqueous solution using different natural adsorbent is shown in Fig 4. The efficiency of Cr (VI) ion removal was found to increase with adsorbent dosage. The variation of adsorption capacities
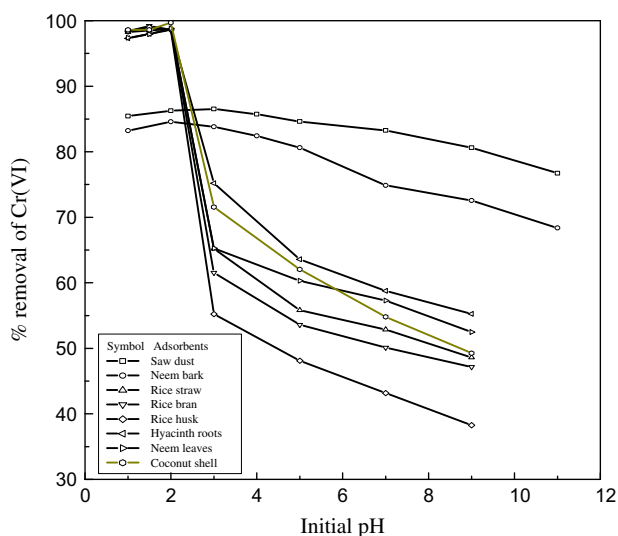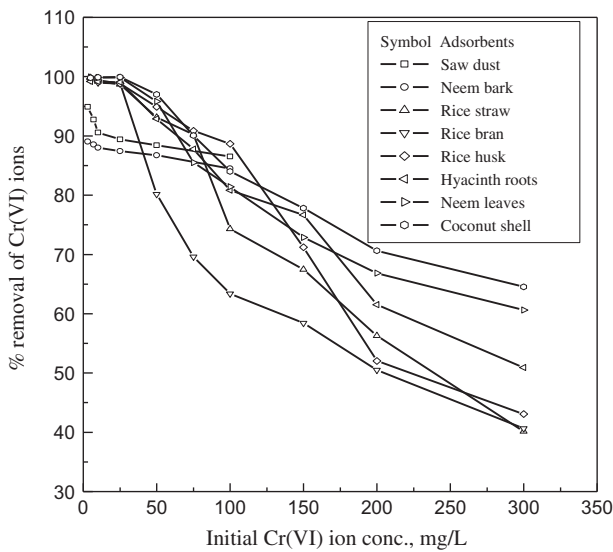
Fig. 3. Effect of initial Cr(VI) ion concentration on the adsorption process (pH: 1.5 for rice husk, 2 for rice straw, rice bran, hyacinth roots, neem leaves, coconut shell, and 3 for saw dust and neem bark; adsorbent dosage: 10 g/L; and contact time: 5 h for saw dust, neem bark, neem leaves, 6 h for coconut shell, 7 h for rice straw, rice bran, rice husk, and hyacinth roots).
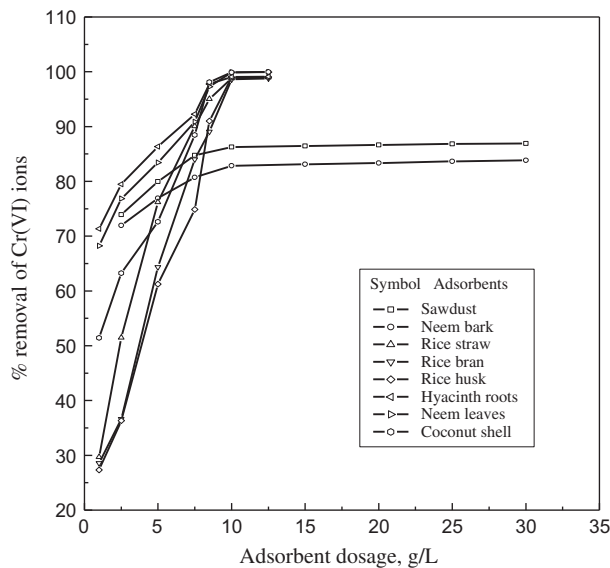
Fig. 4. Effect of adsorbent dosage on the adsorption of Cr (VI) (pH: 1.5 for rice husk, 2 for rice straw, rice bran, hyacinth roots, neem leaves, coconut shell, 3 for saw dust and neem bark; metal concentration: 50 mg/L for saw dust and neem bark, 25 mg/L for other adsorbents; and contact time: 3 h for rice straw, 4 h for saw dust, neem bark, hyacinth roots, neem leaves, coconut shell, 5 h for rice bran, and 6 h for rice husk).

between the different biosorbents could be related to the type and concentration of the functional group responsible for the adsorption of metal ions [7]. With increase in adsorbent dosage, more surface area was available for adsorption due to increase in active sites on the adsorbent. The optimum conditions for the adsorption process are listed in Table 2.

3.2. ANN Performance

Sola and Sevilla [37] reported the effects of data normalization on the ANN process and concluded normalization of data yields better prediction, however, recently, it was reported that better results are

Table 4
Range of variables for batch experiment

Adsorbent	Initial pH	Initial Cr(VI) concentration (mg/L)	Contact time (min)	Adsorbent dosage (g/L)
Saw dust	2–11	3–300	0–300	2.5–30.0
Neem bark	2–11	3–300	0–300	2.5–30.0
Rice straw	1–9	5–300	0–420	2.5–12.5
Rice bran	1–9	5–300	0–420	2.5–12.5
Rice husk	1–9	5–300	0–420	2.5–12.5
Hyacinth roots	1–9	5–300	0–420	2.5–12.5
Neem leaves	1–9	5–300	0–300	2.5–12.5
Coconut shell	1–9	5–300	0–360	2.5–12.5
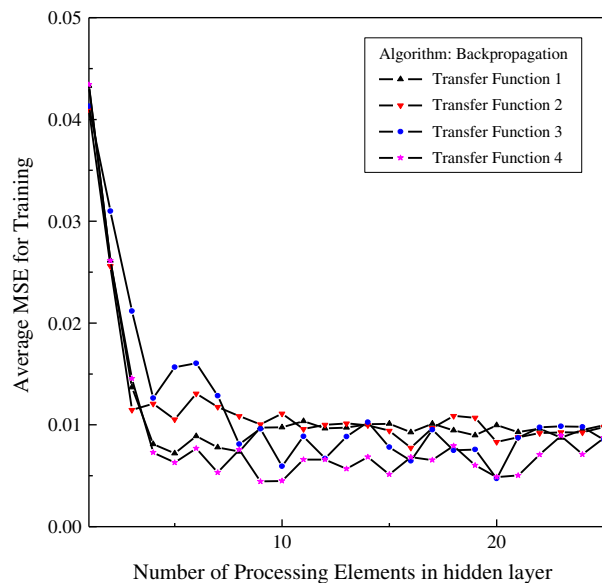
Fig. 5. Variation of MSE for cross-validation with the number of nodes for different transfer functions.
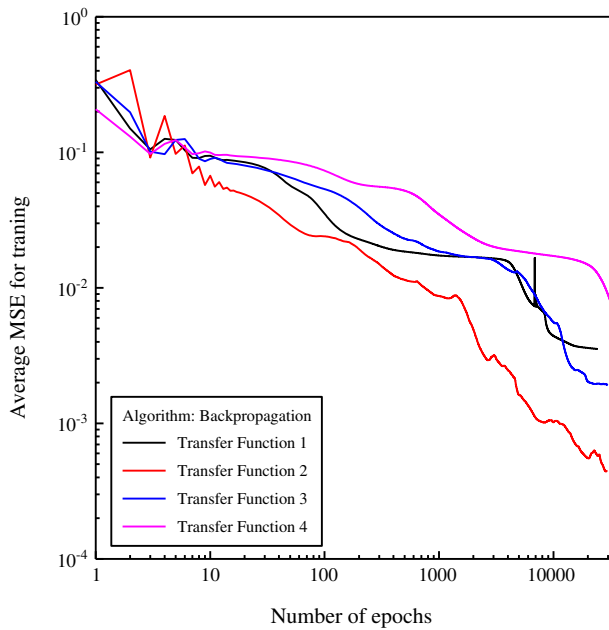
Fig. 6. Variation of the MSE for training vs. the number of epochs.
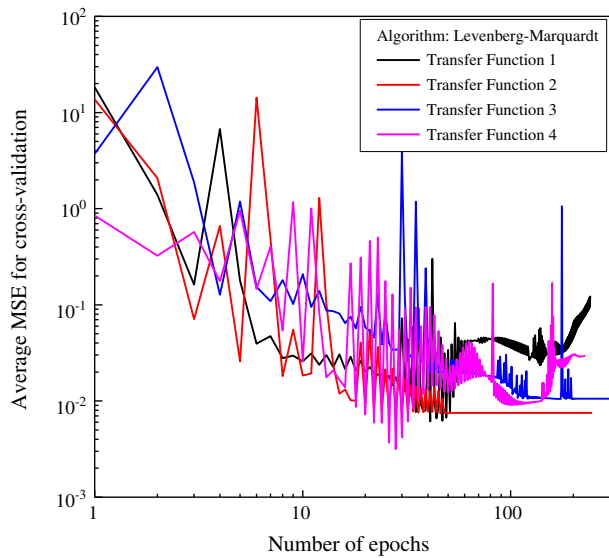
Fig. 7. Variation of the MSE for cross-validation vs. the number of epochs.

yielded without normalization also [38]. Hence, in this case, all raw data are used as input variables without normalization. Table 4 represents the range of variables investigated as input variables and the total number of data points is 163. The performance of the network is checked using the following parameters:

Mean square error (MSE),

$$MSE = \frac{1}{N}\sum_{i=1}^{N}(y_i - y_i^*)^2 \qquad (6)$$

Average absolute relative error (AARE),

$$AARE = \frac{1}{N}\sum_{i=1}^{N}\left|\frac{(y_i^* - y_i)}{y_i}\right| \qquad (7)$$

Standard deviation (σ),

$$\sigma = \sqrt{\sum_{i=1}^{N}\frac{1}{N-1}\left[\left|\frac{(y_i^* - y_i)}{y_i}\right| - AARE\right]^2} \qquad (8)$$

Cross-correlation coefficient (R),

$$R = \frac{\sum_{i=1}^{N}(y_i - \overline{y})(y_i^* - \overline{y^*})}{\sqrt{\sum_{i=1}^{N}(y_i - \overline{y})^2 \sum_{i=1}^{N}(y_i^* - \overline{y^*})^2}} \qquad (9)$$

Chi-square test (χ^2),

$$\chi^2 = \sum_{i=1}^{N}\frac{(y_i - y_i^*)^2}{y_i^*} \qquad (10)$$

For better performance of the network, the MSE, AARE, and standard deviation should be as small as possible. It has also been verified that the cross-correlation coefficient between input and output should be close to unity for better predictability. When more than one model is acceptable statistically, then the Chi-square test should be performed to find the best-fit model. The lowest value indicates the best model.

Fig. 5 shows the variation of MSE with the number of nodes for different transfer functions when BP algorithm was used in both hidden and output layer. A

Table 5
Minimum value of cross-validation MSE during training with four different transfer functions

Algorithm	Measurement type	Transfer function 1	Transfer function 2	Transfer function 3	Transfer function 4
BP	MSE	0.007190	0.007749	0.004738	0.004433
LM		0.006140	0.007422	0.010450	0.003146

Table 6
Performance of neural network with different transfer functions for testing using optimum number of processing elements

Algorithm	Measurement type	Transfer function 1	Transfer function 2	Transfer function 3	Transfer function 4
BP	AARE	0.055300	0.088058	0.053861	0.063896
	SD (σ)	0.040302	0.093480	0.040821	0.046964
	MSE	20.28852	47.75586	26.70847	30.60503
	CCC (R)	0.967442	0.913026	0.954456	0.952915
LM	AARE	0.062204	0.056555	0.070699	0.049624
	SD (σ)	0.050772	0.044129	0.062844	0.032542
	MSE	26.79431	22.99827	33.64374	18.71493
	CCC (R)	0.956842	0.961997	0.949956	0.968771
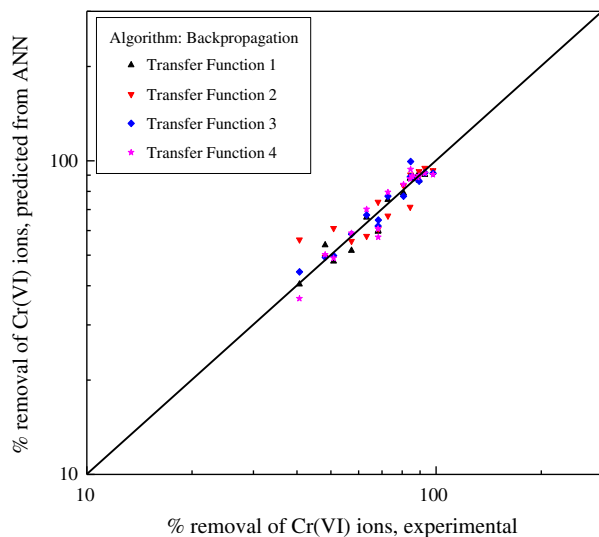
Fig. 8. Comparison of percentage removal for ANN prediction and experimental results with four different transfer functions in the hidden layer for testing.

similar procedure was followed for training with LM algorithm. The optimum number of nodes is the one where the MSE for cross-validation is minimum. Fig. 6 represents the training curve of the neural networks when BP algorithm was used. The optimum number of processing element is estimated on the basis of minimum value of MSE for cross-validation. Fig. 7 represents the cross-validation curve of the neural networks when LM algorithm was used. Initially, the MSE for each epoch for training and cross-validation in both cases are recorded for five different runs separately. There were two stopping criteria for the training of the network. If there is no improvement in the value of cross-validation MSE for 20,000 epochs, then the training was set to stop. For training with both the algorithms, the minimum value of MSE of cross-validation (the threshold value) was set at 0.001 for all the four different transfer functions in the hidden layer. For the hidden layer of BP network, the

Table 7
Performance of neural network with different transfer functions for prediction using optimum number of processing elements

Algorithm	Measurement type	Transfer function 1	Transfer function 2	Transfer function 3	Transfer function 4
BP	AARE	0.077706	0.078630	0.089642	0.073617
	SD (σ)	0.135561	0.084056	0.093446	0.078303
	MSE	45.79378	46.34546	46.44381	30.93147
	CCC (R)	0.943763	0.952204	0.953545	0.962527
	χ^2	11.41718	13.41852	13.37263	8.771089
LM	AARE	0.097346	**0.068778**	0.116993	0.075846
	SD (σ)	0.127050	**0.072029**	0.124751	0.082228
	MSE	53.68315	**30.43068**	70.49896	33.03687
	CCC (R)	0.935763	**0.962237**	0.917787	0.963493
	χ^2	17.82163	**8.390167**	22.86298	10.40875

Table 8
Description of weights associated with input, hidden, and output layers

Serial no.	Input to hidden layer connection				Output to hidden layer connection
1	0.004093	0.307667	0.711721	−0.667327	0.490202
2	−0.252397	0.216979	−0.718551	−1.453808	−0.777557
3	−0.355136	−0.078038	0.079612	0.436439	0.905247
4	0.576476	−0.049406	0.268346	0.372066	−0.145048
5	−0.210925	−0.183375	−0.437285	−0.586537	−0.535508
6	1.083122	0.294503	0.001665	0.847319	1.111713
7	0.058674	−0.374346	0.365316	−0.863709	−0.323758
8	1.286735	−0.035538	1.482840	−0.420459	−0.609782
9	−0.209066	−0.773105	−0.108152	−0.114437	1.129915
10	0.960628	0.372893	−1.134731	0.006170	−0.008940
11	0.295896	−0.697492	0.333204	−0.093179	−0.272155
12	0.338536	−3.089213	1.182684	0.203710	0.068179
13	0.461557	−0.664719	0.380643	−0.387884	−0.807871
14	−0.388255	−0.190040	−0.018621	0.464077	0.855634
15	0.504177	1.496818	−0.050444	−0.180411	−0.590328
16	−0.056421	−0.665780	0.005551	0.057835	0.525473
17	−0.765281	−0.779470	0.127195	0.027548	−0.202252
18	0.280103	0.137721	−0.506341	−0.305682	−0.393473
19	0.541006	−1.514863	−1.045546	1.377181	−0.460895
20	−0.025035	−0.001037	1.424022	0.738552	−0.392533
21	2.898609	0.326398	0.280763	−0.168228	−0.253040

value of learning rate was 0.7 and that of momentum coefficient was 1. Table 5 represents the minimum value of cross-validation MSE reached during training with four different transfer functions for training with both the algorithms. A similar type of procedure was also reported in our earlier works [30,31].

Testing was done just before the final prediction to check the effectiveness of training using the above-mentioned four networks. Table 6 represents the performance of the testing. The low values of AARE and cross correlation co-efficient (R), which is greater than 0.91 in each case indicates that the training was good and the network can be used for final prediction. Fig. 8 shows the comparison between the experimental to the predicted percentage removal with optimum number of processing elements in the hidden layer for testing.

Table 7 represents the performance of the neural networks for final prediction. It is clear from the table that the cross correlation co-efficient (R) value is nearly 0.95 for each of the four cases. The low value of the average absolute relative error (AARE) also shows the accuracy of the result in the different systems. From these observations, it is clear that the ANN trained with both the algorithms predict the percentage removal well.

The high value of cross-correlation co-efficient (R) and the low value of chi square (χ^2) for the transfer function 2 with 21 (optimum number) processing
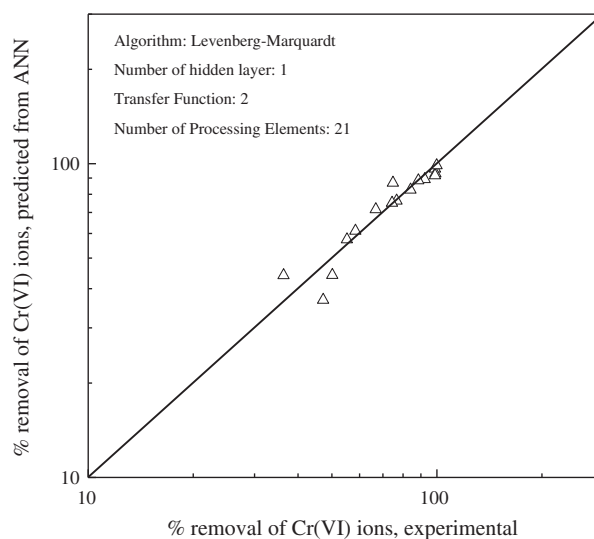
Fig. 9. Comparison of percentage removal for ANN prediction and experimental results with nine processing elements and Transfer function 4 in the hidden layer for final prediction.

Table 9
Comparison of the experimental and ANN-predicted percentage removal of Cr(VI)

Name of adsorbent	Initial pH	Initial Cr(VI) concentration (mg/L)	Contact time (min)	Adsorbent dosage (g/L)	Percentage removal of Cr(VI)	
					Experimental	ANN prediction
Neem bark	3	7	240	10	88.53	88.44
Rice straw	2	25	180	10	98.80	91.89
	2	100		10	74.32	74.99
Rice bran	2	150	300	10	58.43	61.12
	7	25		10	50.12	44.18
	9	25		10	47.17	36.83
Rice husk	1.5	25	360	2.5	36.33	44.10
	1.5	25		7.5	74.87	87.01
Hyacinth roots	2	10	240	10	99.15	93.15
	2	25		7.5	92.25	89.24
	2	150		10	76.65	76.21
	9	25		10	55.26	57.40
Neem leaves	2	25	240	10	98.81	96.38
	2	200		10	66.83	71.62
	2	5		10	99.92	98.79
Coconut shell	2	100	240	10	84.01	82.68

elements (when the network was trained with LM algorithm) gives the most accurate prediction of the percentage removal.

The weights associated with this network having 21 processing elements of the hidden layer connected to each of the four inputs (84 connections in total, i.e. 21 each for the four inputs) and also connected to the output (21 connections in total) are presented in Table 8.

Fig. 9 and Table 9 show the comparison between the experimental to the predicted percentage removal with 21 processing elements and transfer function number 2 in a hidden layer when the network was trained with LM algorithm. This result indicates that the performance of the network output is excellent.

4. Conclusion

A neural network based model was developed for the prediction of percentage removal. A multilayer perceptron with BP and LM algorithm were used for the analysis. Four different slandered transfer functions in a hidden layer and a linear output function were used. Optimization for each transfer function was carried out in all cases. The ANN model trained with LM algorithm using a hidden layer with transfer function 2 and 21 processing elements gives better predictability of the percentage removal.

Acknowledgment

References

[1] A.K. Bhattacharya, S.N. Mandal, S.K. Das, Adsorption of Zn (II) from aqueous solution by using different adsorbents, Chem. Eng. J. 123(1–2) (2006) 43–51.
[2] E. Malkoc, Y. Nuhoglu, Y. Abali, Cr(VI) adsorption by waste acorn of Quercus ithaburensis in fixed beds: Prediction of breakthrough curves, Chem. Eng. J. 119(1) (2006) 61–68.
[3] N. Hsu, S. Wang, Y. Liao, S. Huang, Y. Tzou, Y. Huang, Removal of hexavalent chromium from acidic aqueous solutions using rice straw-derived carbon, J. Hazard. Mater. 171 (1–3) (2009) 1066–1070.
[4] B. Singha, S.K. Das, Biosorption of Cr(VI) ions from aqueous solutions: Kinetics, equilibrium, thermodynamics and desorption studies, Colloids Surf., B 84 (2011) 221–232.
[5] EPA (Environmental Protection Agency), Environmental pollution control alters, EPA/625/5-90/025, EPA/625/4- 89/ 023, Cincinnati, 1990.
[6] MINAS, Pollution control acts, rules, and notification there under central pollution control board, 2001, Ministry of Environment and Forests, Government of India, New Delhi, 2001.
[7] T.K. Naiya, P. Chowdhuary, A.K. Bhattacharya, S.K. Das, Saw dust and neem bark as low-cost natural biosorbent for adsorptive removal of Zn(II) and Cd(II) ions from aqueous solutions, Chem. Eng. J. 148(1) (2009) 68–79.
[8] R. Plippman, An introduction to computing with neural nets, IEEE ASSP Mag. 4 (1987) 4–22.
[9] S. Haykin, Neural Networks—A Comprehensive Foundation, 2nd ed., Prentice-Hall, USA, 1999.
[10] L.M. Fu, Neural Networks in Computer Intelligence, McGraw Hill, New York, 1994.

[11] E. Barnard, L. Wessels, Extrapolation and interpolation in neural network classifiers, IEEE Control Syst. 12(5) (1992) 50–53.

[12] H. White, Connectionist nonparametric regression: Multilayer feed-forward networks can learn arbitrary mapping, Neural Networks 3 (1990) 535–549.

[13] S. Walczak, Developing neural nets currency trading, Artif. Intel. Finance 2(1) (1995) 27–34.

[14] A. Bansal, R.J. Kanuffman, R.R. Weitz, Comparing the modeling performance of regression and neural networks as data quality varies: A buisnessvalue approach, J. Manage. Inform. Syst. 10(1) (1993) 11–32.

[15] S. Tamura, M. Tateishi, Capabilities of four layered feedforward neural network: Four layers versus three, IEEE Trans. Neural Networks 8(2) (1997) 251–255.

[16] N.G. Turan, B. Mesci, O. Ozgonenel, The use of artificial neural networks (ANN) for modeling of adsorption of Cu(II) from industrial leachate by pumice, Chem. Eng. J. 171 (2011) 1091–1097.

[17] N.G. Turan, B. Mesci, O. Ozgonenel, Artificial neural networks (ANN) approach for modeling Zn(II) adsorption from leachate using a new biosorbent, Chem. Eng. J. 173 (2011) 98–105.

[18] A.K. Bhattacharya, T.K. Naiya, S.N. Mondal, S.K. Das, Adsorption, kinetics and equilibrium studies on removal of Cr(VI) from aqueous solutions using different low-cost adsorbents, Chem. Eng. J. 137(3) (2008) 529–541.

[19] B. Singha, S.K. Das, Biosorption of Cr(VI) ions from aqueous solutions: Kinetics, equilibrium, thermodynamics and desorption studies, Colloids Surf., B 84 (2011) 221–232.

[20] V.C. Srivastava, I.D. Mall, I.M. Mishra, Characterization of mesoporous rice husk ash (RHA) and adsorption kinetics of metal ions from aqueous solution onto RHA, J. Hazard. Mater. 134 (2006) 257–267.

[21] APHA, AWWA, WEF, Standard Methods for Examination of Water and Wastewater, 20th ed., Washington DC, New York, 1998.

[22] F. Soulié, Integrating neural networks for real world applications, In: J.M. Zurada, R.J. Marks, C.J. Robinson (Eds.), Computational Intelligence : Imitating Life, IEEE Press, New York, pp. 396–405, 1994.

[23] R. Pakath, J.S. Zaveri, Specifying critical inputs in a genetic algorithm-driven decision support system: An animated facility, Decis. Sci. 26 (1995) 749–779.

[24] S. Walczak, N. Cerpa, Hauristic principles for the design of artificial neural networks, Inform. Software Technol. 41 (1999) 107–117.

[25] S. Walczak, Categorizing university student applicants with neural networks, Proc. IEEE Int. Conf. Neural Networks, 1994, pp 3680–3685.

[26] C. Kon, J. Shih, C. Lin, Z. Lee, An application of neural networks to reconstruct crime scenebased on non-Mark theory—suspicious factors analysis, in: P.K.Simpson (Ed.), Neural Networks : Theory, Technology and Applications, IEEE Press, New York, 1996, p. 537.

[27] M. Smith, Neural Networks for Statistical Modeling, Van Nostrand Reinhold, New York, 1993.

[28] M.J. Lenard, P. Alam, G.R. Madey, The application of neural networks and a qualitative response model to the auditor's going concern uncertainly decision, Decisi. Sci. 26(2) (1995) 209–227.

[29] B.A. Jain, B.R. Nag, Artificial neural network models for pricing initial public offerings, Decisi. Sci. 26(3) (1995) 283–302.

[30] N. Bar, S.K. Das, Comparative study of friction factor by prediction of frictional pressure drop per unit length using empirical correlation and ANN for gas-non-Newtonian liquid flow through 180˚ circular bend, Int. Rev. Chem. Eng. 3(6) (2011) 628–643.

[31] N. Bar, S.K. Das, Gas-non-newtonian liquid flow through horizontal pipe—gas holdup and pressure drop prediction using multilayer perceptron, Int. Rev. Chem. Eng. 2(3) (2012) 7–16.

[32] M. Bansal, U. Garg, D. Singh, V.K. Garg, Removal of Cr(VI) from aqueous solutions using pre-consumer processing agricultural waste: A case study of rice husk, J. Hazard. Mater. 162(1) (2009) 312–320.

[33] P. Miretzkya, A. F. Cirelli, Cr(VI) and Cr(III) removal from aqueous solutions by raw and modified lignocellulosic materials: A review, J. Hazard. Mater. 180 (2010) 1–19.S.

[34] Mallick, S. S. Dash, K. M. Parida, Adsorption of hexavalent chromium on manganese nodule leached residue obtained from NH3-SO3 leaching, J. Colloid Interface Sci. 297 (2006) 419–425.

[35] K. Kadirvelu, C. Namasivayam, Activated carbon from coconut coir pitch as metal adsorbent: Adsorption of Cd(II) from aqueous solution, Adv. Environ. Res. 7 (2003) 471–478.

[36] A.K. Bhattacharya, T.K. Naiya, S.N. Mandal, S.K. Das, Adsorption, kinetics and equilibrium studies on the removal of Cr(VI) from aqueous solutions using different low-cost adsorbents, Chem. Eng. J. 137(3) (2008) 529–541.

[37] J. Sola, J. Sevilla, Importance of input data normalization for the application of neural networks to complex industrial problems, IEEE Trans. Nuclear Sci. 44(3) (1997) 1464–1468.

[38] Wu. Guan-De, Shang-Lien Lo, Effects of data normalization and inherent-factor on decision of optimal coagulant dosage in water treatment by artificial neural network, Expert Syst. App. 37(7) (2010) 4974–4983.